Slow Inactivation Does Not Block the Aqueous Accessibility to the Outer Pore of Voltage-gated Na Channels

Arie F. Struyk[1] and Stephen C. Cannon[1,2]

[1]Department of Neurology, Massachusetts General Hospital, and [2]Department of Neurobiology, Harvard Medical School, Boston, MA 02114

ABSTRACT Slow inactivation of voltage-gated Na channels is kinetically and structurally distinct from fast inactivation. Whereas structures that participate in fast inactivation are well described and include the cytoplasmic III-IV linker, the nature and location of the slow inactivation gating mechanism remains poorly understood. Several lines of evidence suggest that the pore regions (P-regions) are important contributors to slow inactivation gating. This has led to the proposal that a collapse of the pore impedes Na current during slow inactivation. We sought to determine whether such a slow inactivation-coupled conformational change could be detected in the outer pore. To accomplish this, we used a rapid perfusion technique to measure reaction rates between cysteine-substituted side chains lining the aqueous pore and the charged sulfhydryl-modifying reagent MTS-ET. A pattern of incrementally slower reaction rates was observed at substituted sites at increasing depth in the pore. We found no state-dependent change in modification rates of P-region residues located in all four domains, and thus no change in aqueous accessibility, between slow- and nonslow-inactivated states. In domains I and IV, it was possible to measure modification rates at residues adjacent to the narrow DEKA selectivity filter (Y401C and G1530C), and yet no change was observed in accessibility in either slow- or nonslow-inactivated states. We interpret these results as evidence that the outer mouth of the Na pore remains open while the channel is slow inactivated.

KEY WORDS: gating • cysteine-scanning mutagenesis • methanthiosulfonate • NaV1.4

INTRODUCTION

Voltage-gated Na channels in excitable tissues undergo two types of inactivation that are easily distinguishable by their different kinetics. Fast inactivation, which helps terminate the action potential and sets the refractory period, occurs over a period spanning several milliseconds. Slow inactivation develops in response to prolonged depolarizations of hundreds of milliseconds to seconds or to long trains of brief repetitive depolarizations, and recovers over similarly extended periods. Recently, it has been demonstrated that a number of Na channel point mutations that cause heritable disorders of skeletal muscle membrane excitability, notably hyper- and hypokalemic periodic paralysis, may do so in part by altering the kinetics or voltage dependence of slow inactivation (Cannon, 1996; Cummins and Sigworth, 1996; Hayward et al., 1999; Jurkat-Rott et al., 2000; Struyk et al., 2000; Kuzmenkin et al., 2002), consequently interest has been heightened in the physiological role of this process.

The structures of the voltage-gated Na channel that participate in slow inactivation are not well defined, but are different from those that mediate fast inactivation. Exposure of the cytoplasmic face of the Na channel to proteases (Rudy, 1978) or mutation of the IFM peptide located in the cytoplasmic linker region between domains III and IV (Cummins and Sigworth, 1996; Featherstone et al., 1996), both of which impair fast inactivation, do not disrupt slow inactivation. A number of studies have suggested that structures that together form the outer mouth of the pore, the P-regions lying between the S5 and S6 segments of each of the four Na channel domains, are important for slow inactivation. First, permeant metal cations applied via the external surface can modestly inhibit slow inactivation (Khodorov et al., 1976; Townsend and Horn, 1997). Second, a point mutation in the domain I P-region of the rat skeletal muscle voltage-gated Na channel rSkM1 (W402C) partially disrupts slow inactivation (Balser et al., 1996). Third, substitution of a single amino acid in the domain II P-region of the human cardiac Na channel isoform (hH1) into the comparable residue in the human skeletal muscle–specific isoform (hSkM1) converts hSkM1-type slow inactivation to hH1-type (Vilin et al., 2001). Fourth, in a mutant channel into which a double cysteine substitution in two P-regions has been introduced (K1237C + W1531C), disulfide bond formation between these substituted residues is enhanced when mutant channels are slow inactivated (Benitah et al., 1999). Finally, a residue deep within the domain III P-region is less accessible to covalent modification by an externally applied agent when

Address correspondence to Dr. Stephen C. Cannon at his present address Department of Neurology/F2.318, University of Texas Southwestern Medical Center, 5323 Harry Hines Blvd., Dallas, TX 75390-9036. Fax: (214) 648-6306; E-mail: steve.cannon@utsouthwestern.edu

channels are slow inactivated (Ong et al., 2000). These results have led many to suggest that slow inactivation may involve a conformational rearrangement in the outer mouth of the pore. In this manner, Na channel slow inactivation may be akin to *Shaker* K channel C-type inactivation, in which a collapse of the outer pore-forming segments occludes the aqueous permeation pathway (Liu et al., 1996). However, none of these results directly demonstrate that the Na channel outer vestibule is occluded during slow inactivation. Equally compelling evidence suggests that structures located more internally may also be important in slow inactivation. A growing pattern of missense mutations in the inner pore forming S6 segments, primarily in domains I or IV, variably disrupt or enhance slow inactivation (Wang and Wang, 1997; Takahashi and Cannon, 1999; O'Reilly et al., 2000, 2001; Vedantham and Cannon, 2000). These results suggest that conformational changes in internally oriented pore regions may, in isolation or as part of a global collapse of the pore, be part of slow inactivation gating.

We sought to determine whether a conformational rearrangement consistent with occlusion of the outer pore could be detected during slow inactivation. To do this, we introduced cysteine substitution mutations at amino acid positions in COOH-terminal ascending loops of P-regions lining the pore. A rapidly switched perfusion method was then used to measure reaction rates between these substituted side chains and the charged sulfhydryl-modifying reagent [2-(trimethylammonium) ethyl] methanethiosulfonate (MTS-ET).* Application of MTS-ET was time-locked to specific epochs in a voltage-clamp protocol to test for state-dependent changes in those modification rates between minimally and maximally slow-inactivated channel populations. Cysteine modification rates, as detected by progressive irreversible block with successive MTS-ET applications, were measurable at sites in each of the four P-regions, and in two cases at sites adjacent to the narrow ring of charged residues which form the Na ion selectivity filter (DEKA locus). No differences in MTS-ET modification rates at these sites were observed between conditions favoring fast versus slow inactivation. We interpret these results as evidence that occlusion of the external aqueous permeation pathway to the selectivity filter does not occur during slow inactivation.

MATERIALS AND METHODS

Mutagenesis and mRNA Preparation

The rat adult skeletal muscle Na channel α subunit cDNA (rSkM1, now termed rNaV1.4), subcloned into the EcoRI site of the *Xenopus* expression vector pGEMHE (Liman et al., 1992), was used as a template for an overlapping primer-based PCR mutagenesis method using the QuickChange site-directed mutagenesis kit (Stratgene). Primers were designed to alter codons specifying the cysteine substitution and to introduce a silent restriction enzyme site used for rapid screening by restriction digest. Point mutations were confirmed by sequence analysis through the codon position.

cRNA was synthesized by in vitro transcription from 1.5 μg of Nhe1-linearized vector DNA template using the T7 mMessage mMachine kit (Ambion).

Expression of Na Channels

Xenopus oocytes were harvested and coinjected with either wild-type or mutant NaV1.4 cRNA and a β1 subunit encoding cRNA (McClatchey et al., 1993). Oocytes were incubated for 1–3 d in ND96 medium (in mM: 96 NaCl, 2 KCl, 1.8 $CaCl_2$, 1 $MgCl_2$, 5 HEPES, pH 7.6) supplemented with 2.5 mg/ml pyruvate and 50 μg/ml gentamicin, before use in electrophysiological recording.

Electrophysiology

The vitelline membrane was mechanically dissociated from the oocyte after incubation in hypertonic solution for 5–20 min, before transfer to the recording chamber. Na currents were measured in excised outside-out macropatches with an Axopatch 200B amplifier (Axon Instruments, Inc.). The amplifier output was filtered at 5 kHz and digitally sampled at 20 kHz using a Digi-Data 1200 interface (Axon Instruments, Inc.). Control over the amplifier, digital output to the piezo switching apparatus, and data storage was accomplished with a custom AxoBasic data acquisition program. Pipette capacitance was compensated using analogue circuitry. Linear leakage current correction was performed on-line through digital scaling and subtraction of passive currents elicited by hyperpolarizing voltage pulses from −120 to −145 mV. Patch electrodes were pulled from borosilicate capillary tubes with a two-stage puller (Sutter Instruments Co.). The shanks of the electrode tips were coated with Sylgard and the tips were heat polished to a final tip resistance of 2–4 MΩ.

The pipette (internal) solution contained (in mM): 100 KCl, 10 HEPES, 5 EGTA, 1 $MgCl_2$, pH 7.6 with KOH. The bath (external) solution contained (in mM): 100 NaCl, 10 HEPES, 2 $CaCl_2$, 1 $MgCl_2$, pH 7.6 with NaOH. Stock solutions of MTS-ET at a concentration of 100 mM were made fresh daily in water and placed on ice at the beginning of each recording day. Immediately before use in perfusion experiments, appropriate amounts of MTS-ET were diluted into 5 ml of bath solution (for final concentrations ranging from 100 μM to 8 mM) after suitable patches were obtained.

Rapid solution exchange was achieved as described previously (Vedantham and Cannon, 1998). Briefly, a computer-controlled PZS-200 piezoelectric stack (Burleigh Instruments, Inc.) was used to translocate a piece of glass capillary theta tubing (2.0 mm outer diameter) over a macropatch. The theta tubing was pulled to an internal diameter of 50–100 μm (each lumen) on a two-stage puller. Solutions were passed through each lumen by gravity filtration.

Data Analysis

Curve fitting was performed off-line using AxoBasic or Origin (Microcal). The time course of entry into and recovery from inactivation was examined using a two-pulse protocol as described in the text. For recovery from fast or from slow inactivation, the fractional peak I_{Na} recovery was fit with the single exponential function:

$$I_{test}/I_{reference} = A(1 - e^{-t/\tau}) + y_0,$$

**Abbreviation used in this paper:* MTS-ET, [2-(trimethylammonium) ethyl] methanethiosulfonate.

where $I_{reference}$ is the peak I_{Na} elicited by a depolarizing pulse preceding each conditioning pulse, A is the amplitude of the exponential component, y_0 the fractional I_{Na} at time 0 (i.e., not inactivated), and τ is the time constant. For entry into slow inactivation, the fractional peak I_{Na} was fit with the single exponential decay

$$I_{test}/I_{reference} = Ae^{-t/\tau} + y_0.$$

A is the amplitude of the maximal fraction of channels slow inactivated, y_0 is the fraction of channels not slow inactivated at steady-state, and τ is the time constant.

For modification experiments, peak I_{Na} was first determined by a test pulse to −20 mV before MTS-ET exposure. Patches were then exposed to known concentrations of MTS-ET for intervals described in the text, and allowed to recovery from inactivation before the remaining peak I_{Na} was determined. Curves of sequential peak I_{Na} values plotted against cumulative MTS-ET exposure time were fit with the single exponential decay function

$$I_{peak} = I_{max} - I_{mod}(1 - e^{-t/\tau}),$$

where I_{max} is the maximal peak current before modification, I_{mod} is the steady-state reduction in peak current due to cysteine modification, and τ is the time constant. Reaction rates were then determined by taking the reciprocal of the product of the time constant τ and the MTS-ET concentration.

Error bars represent ± SEM. Statistical significance was determined though a paired *t* test, with confidence parameters of <0.05.

RESULTS

We sought to determine whether a reduction in aqueous accessibility to the outer mouth of a Na channel pore, consistent with a conformational rearrangement in this region, might occur during slow inactivation. The assay was based on comparing the reaction rates of cysteine-substituted residues in the SS2 segments of the P-regions of all four domains to covalent modification with methanethiosulfonate (MTS)-containing reagents, when the channel was either slow inactivated or not slow inactivated.

Our choice of sites to assay was directed by previous experiments of Chiamvimonvat et al. (1996) and Perez-Garcia et al. (1996). Mutant Na channels containing cysteine substitutions at amino acid sites in the ascending limb of P-loops (SS2 segments) show a decline in macroscopic peak I_{Na} after exposure to externally applied MTS reagents, consistent with the notion that covalent modification of pore-lining residues with a bulky moiety impedes Na ion flux. In our study, only the permanently (+) charged reagent MTS-ET was used, because we wished to limit the possibility that access to a cysteine-substituted residue occurred via a pathway other than the aqueous pore. This restriction necessitated the exclusion of five residues lying within or immediately adjacent to the selectivity filter (D400, W756, G1238, K1237, and A1530), which are either inaccessible to MTS-ET, or whose modification does not result in a change in macroscopic Na current (Chiamvimonvat et al., 1996; Perez-Garcia et al., 1996). We also confirmed that prolonged exposure of wild-type Na channels to MTS-ET did not result in any decline in macroscopic I_{Na} (unpublished data). Of the 10 mutants we made, that spanned all four P-regions, informative modification rates were measurable in 6 (E403C, Y401C, E758C, M1240C, G1530C, D1532C; shown schematically in Fig. 1).

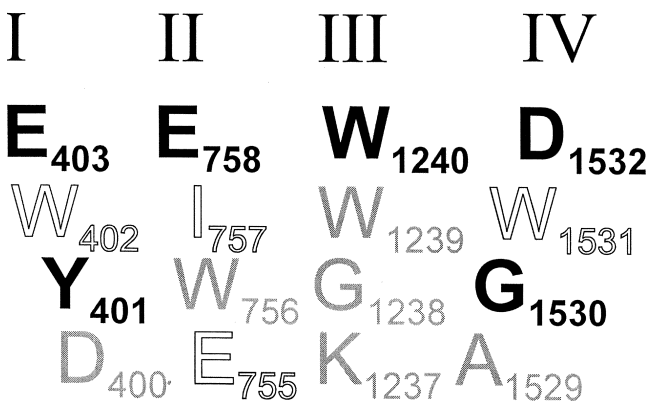

FIGURE 1. Sites of informative cysteine substitution mutations in the outer pore. The SS2 segments are shown schematically in order of relative position from the DEKA Na ion selectivity region. Residues lettered in black represent sites at which cysteine substitution yielded informative data in state-dependent accessibility assays described below. Sites lettered in black outline denote locations at which we were not able to measure a modification rate of substituted cysteine residues. Residues in light gray were not tested, either because they were uninformative since they had no measurable effect when exposed to MTS-ET (D400, W756, K1237, and A1529), they did not produce a detectable I_{Na} (G1238), or the predicted modification rate was too slow for our assay (W1239).

Paired-pulse protocols (detailed in the insets to Figs. 2 and 3) were performed to confirm that the introduction of cysteine residues did not alter the kinetics of fast or slow inactivation in a manner that would impair a mutant's usefulness in our assay. The rate of recovery from fast inactivation at −120 mV (Fig. 2 A) was not altered in any of the mutant channels under study. Similarly, the time course of recovery from slow inactivation at −120 mV, after a 3 s conditioning pulse, was the same for the majority of mutants, although the extent of slow inactivation was reduced for E758C and M1420C (Fig. 2 B and Table I). Recovery from slow inactivation was accelerated modestly for E758C channels ($\tau = 450 \pm 60$, $n = 4$) compared with wild-type channels ($\tau = 640 \pm 40$, $n = 4$).

Entry into slow inactivation at −10 mV (Fig. 3) was not significantly altered for most of the informative mutant channels (E403C, Y401C, G1530C, D1532C). Both E758C and M1240C channels exhibited a modest (~2-fold) prolongation of the entry time constant; however, the difference was statistically significant only for

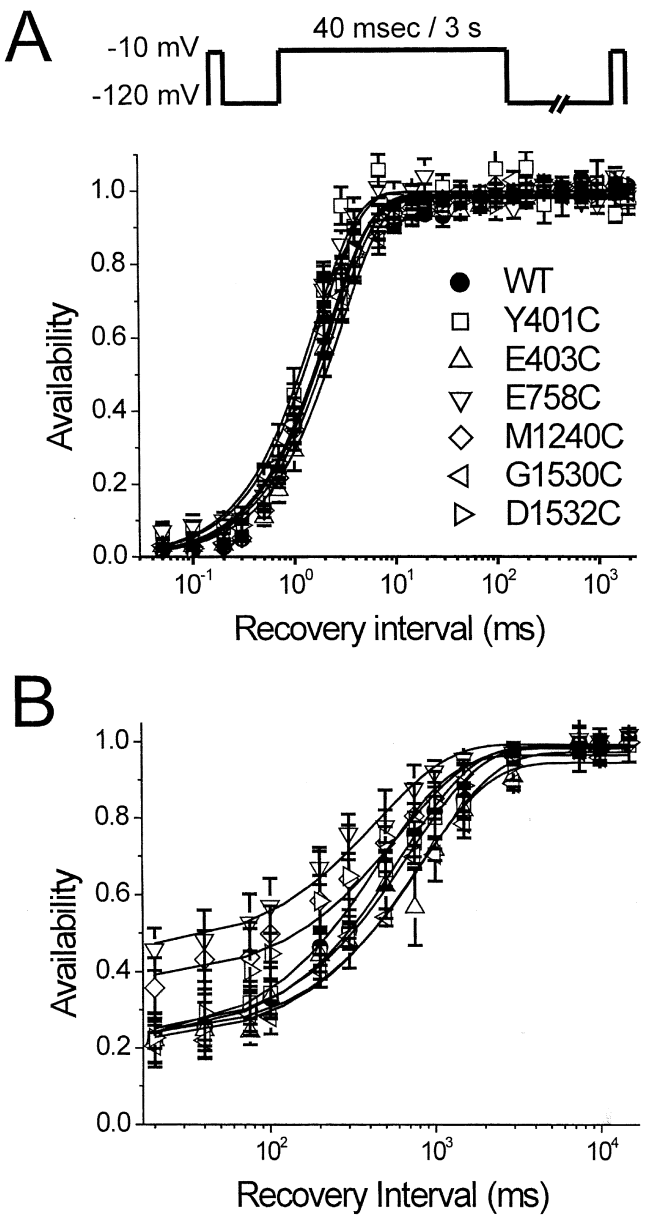

FIGURE 2. Introduction of cysteine missense mutations into informative P-region sites has little or no effect on the recovery kinetics of fast- or slow-inactivation. All measurements were made in excised outside-out macropatches held under perfusion with control bath solution. Conditioning pulses to −10 mV of 40 ms or 3 s duration were used to induce fast and slow inactivation, respectively, (A, inset). (A) Recovery from fast inactivation at −120 mV was unchanged between cysteine substitution mutants and wild-type. (B) Recovery from slow inactivation at −120 mV was not affected by introduction of cysteine residues at most informative sites. For E758C mutant channels, a modest acceleration in the time course of recovery was observed.

E758C. In addition, the steady-state extent of slow inactivation for E758C was reduced compared with wild-type (fraction not slow-inactivated or $S_\infty = 0.19 \pm 0.03$ for E758C and 0.06 ± 0.01 for wild-type). The data summarizing the kinetic behavior of wild-type and mutant channels are listed in Table I.

TABLE I

Comparison of the Kinetic Parameters for Fast and Slow Inactivation

	Fast inactivation		Slow inactivation				
			Entry			Exit	
	$\tau_{recovery}$	n	τ_{entry}	S_∞ (−10 mV)	n	$\tau_{recovery}$	n
	ms		*ms*			*ms*	
Wild-type	2.2 ± 0.18	3	1,000 ± 160	0.06 ± 0.008	3	640 ± 40	4
Y401C	1.6 ± 0.13	4	1,000 ± 170	0.14 ± 0.035	5	710 ± 150	5
E403C	2.9 ± 0.75	6	2,100 ± 500	0.13 ± 0.021	5	890 ± 280	4
E758C	1.8 ± 0.19	4	2,600 ± 380[a]	0.19 ± 0.030[a]	7	450 ± 58[a]	4
M1240C	2.3 ± 0.26	5	2,400 ± 520	0.11 ± 0.025	4	620 ± 130	5
G1530C	2.5 ± 0.57	6	1,600 ± 280	0.07 ± 0.008	6	810 ± 53	4
D1532C	2.2 ± 0.62	3	1,200 ± 130	0.11 ± 0.032	3	470 ± 190	3

[a]$P < 0.04$.

We used these data to design experimental protocols for measuring cysteine accessibility in conditions under which depolarized Na channels are minimally or maximally slow inactivated, shown in Fig. 3. The application of MTS-ET to the extracellular face of an outside-out membrane patch during a specified epoch of the voltage protocol was achieved with millisecond resolution

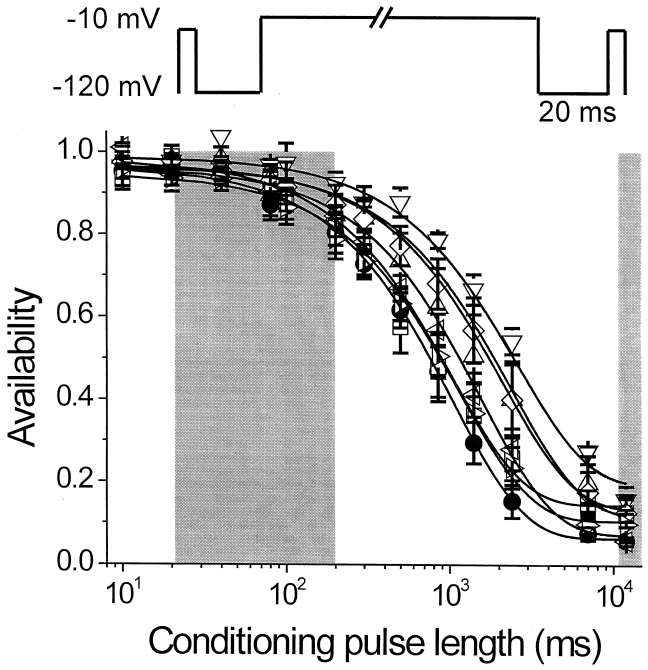

FIGURE 3. The kinetics of entry to slow inactivation at −10 mV. The paired pulse protocol used to measure entry to slow inactivation is shown schematically at the top of the figure. The symbols used for each mutant are identical to those listed in the inset of Fig. 2 A. The majority of the mutations had no significant effect on the time course of entry to slow inactivation. E758C showed a modest 2.5-fold slowing in the time course of entry, and a modest decrease in the maximal extent of slow inactivation (S_∞). The shaded areas represent the timing and duration of the MTS-ET exposures designed to assay cysteine availability for predominantly fast- and slow-inactivated conditions.

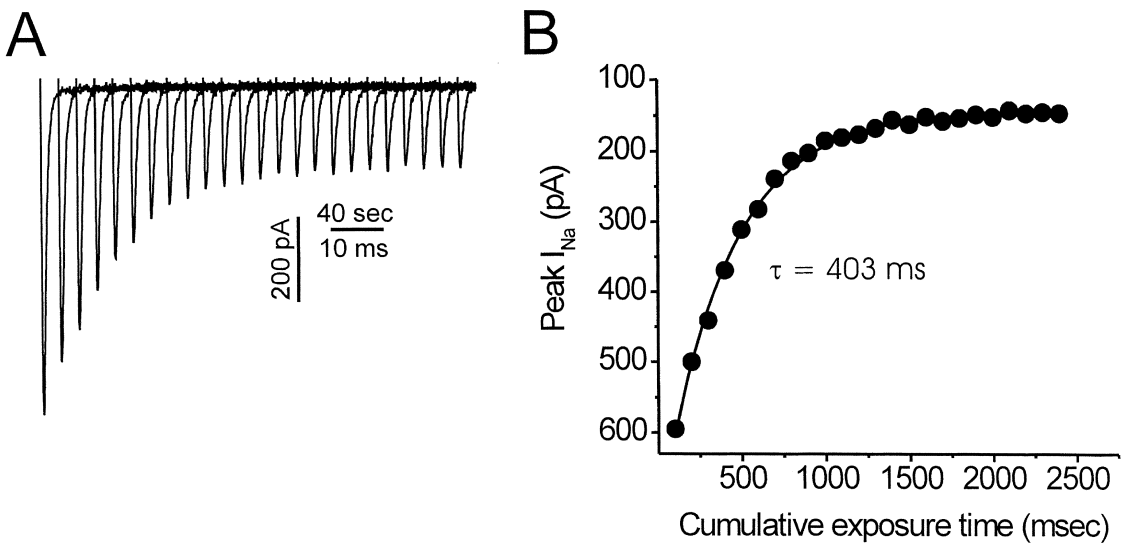

FIGURE 4. Measurement of state-dependent modification rate. (A) Na currents elicited by the assay pulses during serial exposures to MTS-ET are shown on a condensed time scale. The top number of the time scale represents the interval elapsed between each assay pulse, and the bottom number represents the time scale relative to individual assay pulses. In this example, accessibility of the E758C residue is being tested by serial 200 ms exposures to 2 mM MTS-ET early during the conditioning pulse (minimally slow inactivated). (B) Peak I_{Na} values from A are plotted against the cumulative time of exposure to MTS-ET, and fit with a single exponential decay. The apparent modification rate ($R_{Apparent}$) is then computed from the time constant.

by using a rapid-switching perfusion technique (Vedantham and Cannon, 1998). Membrane patches were depolarized to −10 mV for 300 ms to achieve fast inactivation of the Na channels with a limited degree of slow inactivation (<20%, Fig. 3), or for 12 s to achieve maximal slow inactivation. During these depolarizing pulses, patches were exposed to MTS-ET for either 100–200 ms (after a 20 ms delay) to assay cysteine side-chain accessibility while the channels were fast- but not slow-inactivated, or for 500–1,000 ms after 10.5 s of depolarization to assay cysteine accessibility during maximal slow inactivation. The extent of modification was monitored after each brief exposure as the progressive decrement in peak I_{Na} elicited by a test pulse to −20 mV after full recovery from the inactivated state (10 s at −120 mV). The modest alterations in slow inactivation kinetics we found in E758C channels did not impair their usefulness in this standardized assay.

An example of the resultant progressive reduction in peak I_{Na} after each exposure is shown on a condensed time scale in Fig. 4 A. The peak I_{Na} measured after each exposure was plotted against cumulative exposure time and subsequently fit to a monoexponential decay whose time constant is linearly related to the product of the modification rate and the concentration of MTS-ET used in the assay (Fig. 4 B). Consistent with results reported by previous authors (Chiamvimonvat et al., 1996; Perez-Garcia et al., 1996), macroscopic I_{Na} is reduced but not eliminated by complete MTS-ET modification since Na permeability is incompletely blocked by the modifying moiety at these sites.

No significant differences were noted in the apparent cysteine-modification rates determined under conditions favoring fast inactivation in comparison to conditions favoring maximal slow inactivation, as shown graphically in Fig. 5. Mean values of the modification rates determined at each site under both conditions are listed in Table II. Mutant E758C had a trend toward a modest increase in the rate of cysteine modification for slow inactivated channels, which did not achieve statistical significance.

For W402C, I757C, E755C, and W1531C channels, we did not observe a progressive decline in peak current, even after many (30–40) pulsed applications of 4 mM MTS-ET to either fast-inactivated (Fig. 6) or slow-inactivated channels (unpublished data). These same cysteine-substituted sites were reported previously to be modifiable by MTS-ET, manifested as significant (>50%) declines in peak I_{Na} (Chiamvimonvat et al., 1996; Perez-Garcia et al., 1996). This discrepancy is most likely due to the lower limit on the detectable rate of modification in our protocol. The slowest modification rate we can observe is ~10 M^{-1} s^{-1}, since slower reaction rates would require very high (>10 mM) concentrations of MTS-ET, and cumulative application times of >10 s. These extreme conditions are precluded by instability of membrane patches under such prolonged perfusion. Taken in the context of previous observations with these mutant channels, our data suggest that although these residues are available for eventual covalent modification by MTS-ET, the rate at which this modification proceeds is slower than the technical limits of our assay.

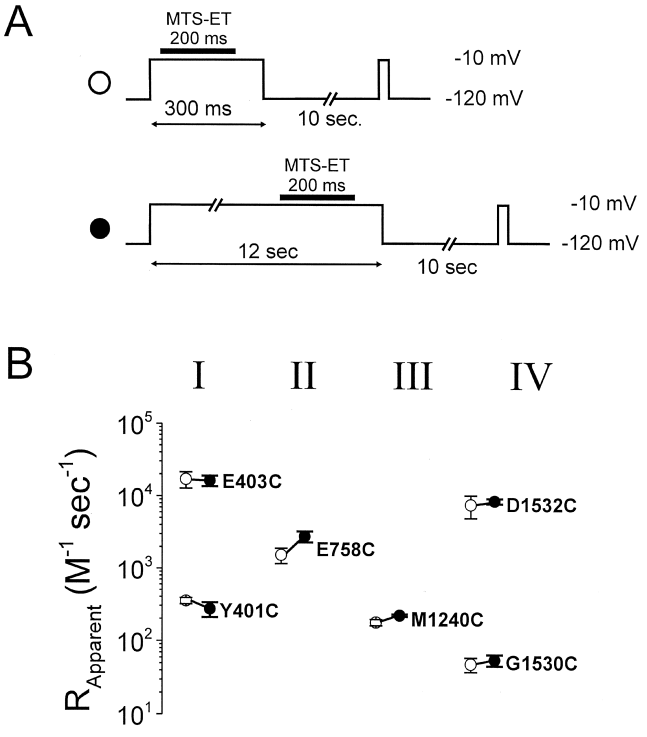

FIGURE 5. No state-dependent change of cysteine modification rate was seen in the six mutants studied. (A) Schematic representation of the pulsed MTS-ET application protocols. Modification rates for fast-inactivated channels were assayed by exposing outside-out patches to MTS-ET for 200 ms, beginning 20 ms into the 300 ms conditioning pulse (top protocol, open circles). To measure the modification rate of slow-inactivated channels, patches were exposed to MTS-ET beginning 10.5 s after the onset of a 12 s conditioning pulse (bottom protocol, filled circles). All conditioning pulses were to −10 mV, and a gap of 10 s at −120 mV to allow for full recovery from inactivation was inserted before a test pulse to −20 mV to measure remaining peak I_{Na}. This cycle was repeated until maximal modification in each patch had taken place. (B) Comparison of modification rates of cysteines in each of the four domains measured under conditions in which channels were predominantly fast- or slow-inactivated. The mean and SEM of these rates are plotted by domain location for each mutant, with rates for the two states of the channel connected by a line. The numerical values are listed in Table II.

TABLE II

Substituted Cysteine Modification Rates in Conditions Favoring Fast or Slow Inactivation

Mutant	Fast inactivated	*n*	Slow inactivated	*n*
	$M^{-1}s^{-1}$		$M^{-1}s^{-1}$	
Y401C	350 ± 35	8	270 ± 63	4
E403C	17,000 ± 4,300	5	16,000 ± 2700	4
E758C	1,600 ± 380	4	2,800 ± 490	5
M1240C	180 ± 17	3	220 ± 8.8	3
G1530C	49 ± 11	5	56 ± 9.8	3
D1532C	7,700 ± 2,600	4	8,700 ± 720	5

DISCUSSION

The conformational changes that produce slow inactivation of voltage-gated Na channels have not been well delineated. Several lines of evidence have implicated a role for the P-region itself (as well as other domains) in this gating process. We searched for evidence of a local rearrangement at the extracellular mouth of the pore by measuring the state-dependent accessibility of cysteines substituted along the ascending limb of the P-loops from all four domains of rNaV1.4 to modification by MTS-ET. Six informative residues, spanning all four domains, were identified, but none showed a substantial change in the rate of modification by MTS-ET for fast- versus slow-inactivated states. This observation suggests the transition from fast- to slow-inactivated states is not accompanied by a major rearrangement in the external mouth of the pore.

The modifiable cysteine-scanning technique cannot exclude the possibility of any movement; only those motions that change the modification rate of the thiol side chain are detectable. Despite these restrictions, our data do provide the first demonstration of a maintained accessibility in slow-inactivated channels to sites very deep within the outer permeation pathway (flanking the DEKA selectivity filter) to MTS-ET, which occupies a cylindrical volume with a 6 Å diameter and 10 Å length (Karlin and Akabas, 1998). We propose this result excludes the notion slow inactivation occurs by occlusion of the outer pore that would block Na ions from reaching the DEKA filter.

The lack of state-dependent differences in MTS-ET modification rates raises the question of whether the technique was sensitive enough to be informative. We offer the following arguments to support our view that had a state-dependent change in thiol accessibility occurred, it would have been detected. First, the modification rates at the informative residues span over two orders of magnitude (Fig. 5). Thus, there was a sufficient dynamic range of measurable rates to detect a change. Second, there is precedent for large changes in modification rate for channels that do undergo state-dependent molecular rearrangements of the outer pore. C-type inactivation of Shaker K channels changes the modification rate of outer pore residues by MTS reagents by 100–10,000 fold (Liu et al., 1996). Third, we have shown previously that state-dependent changes in thiol modification rate as small as fivefold can be robustly demonstrated with our technique (Vedantham and Cannon, 1998), including rate changes within IVS6 produced by slow inactivation (Vedantham and Cannon, 2000). Fourth, the ability of mutant channels to become slow inactivated was verified experimentally for each cysteine substitution (Fig. 3). In quantitative terms, the observable fold-change in apparent modification rate equals the true ratio of modification rates for slow- and not slow–inactivated channels, scaled by the relative occupancy of the slow-inactivated state under our experimental conditions. At the end of the 10 s conditioning pulse, ~80% of channels were slow

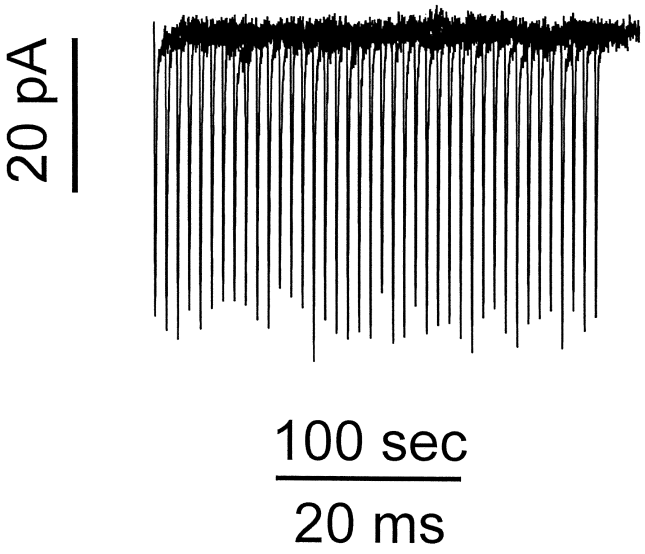

FIGURE 6. Absence of detectable modification of I757C by MTS-ET. Na currents elicited after successive exposures to 4 mM MTS-ET are shown on a compressed time scale. MTS-ET was applied for 200 ms, beginning 20 ms after the onset of a conditioning pulse to −10 mV (fast-inactivation protocol). No reduction in peak I_{Na} was detectable, even after a cumulative exposure time of 8 s. Onset of each trace is offset by the time interval between each trial (scale bar, top). Time scale during a trace is indicated by the number below the scale bar.

inactivated (Fig. 3), and therefore any real change in modification is expected to be observable.

The variation in modification rates we observed for different residues within one P-loop is consistent with contemporary models for the conformation of the pore. In the P-loops of domains I and IV, we were able to measure cysteine modification rates at two positions, including sites adjacent to the DEKA selectivity filter. A marked slowing of modification rate, and thus poorer accessibility, occurred at sites located deeper within the pore along a single segment: rate for E403C was 50-fold faster than Y401C; and D1532C was 150-fold faster than G1530C. Interestingly, no evidence for MST-ET modification was observed at the cysteine substituted at the intervening residue, in either domain I (W402C) or domain IV (W1531C). Because others have reported effects from several minutes long exposure to MTS-ET at these residues (Chiamvimonvat et al., 1996; Perez-Garcia et al., 1996), we infer the modification rate was too slow to measure by our technique. The residues at comparable depths within the pore in domains II (I757) and III (W1239) were similarly too slow to measure. Previously, the accessibility of all of these sites to externally applied MTS reagents was used as evidence that these residues must face into the pore (Perez-Garcia et al., 1996). This accessibility, however, is the result of prolonged (minutes long) exposures of the external membrane surface to MTS-containing solutions. By contrast, our data suggests that accessibility, when characterized by modification rate, is very different between these sites. A recently proposed structural model of the Na channel outer pore, which in turn is extrapolated from the crystal structure of the bacterial KSCA channel, suggests that the SS1 and SS2 segments of the P-regions form a helix-turn-β strand conformation, with the turn occurring at or very near to the residue contributing to the selectivity filter (Lipkind and Fozzard, 2000). Although our data are insufficient to provide support for this entire model, the alternating pattern of accessibility that we observed in P-regions of domains I and IV is consistent with the notion that the pore-lining portions of the SS2 segments are positioned in a β-strand conformation.

Large differences in accessibility to cysteine-substituted sites at roughly similar positions with respect to the selectivity filter were also observed between each of the four domains. For instance, the modification of M1240C proceeds very slowly, regardless of state-population, in comparison to modification at similar sites located in other domains, despite the fact that these residues are spaced equally from the residues comprising the DEKA selectivity locus. These differences do not parallel the relative depths within the electric field these residues occupy (Chiamvimonvat et al., 1996; Perez-Garcia et al., 1996). The reasons for this domain difference is not clear, but may reflect differences in the local microenvironment of these sites, such as altered charge density, hydrophobicity, or spatial impediments to accessing a particular site.

In contrast to the data we present here on the external access pathway to the pore, prior reports suggest that the structural integrity of the P-regions is important for normal slow inactivation. Cysteine substitution at the W402 site in rNaV1.4 can impede entry into an early slow inactivation state (I_M) (Balser et al., 1996). Chimeric substitution of the isoleucine at position 891 in the domain II P-region of the human cardiac muscle Na channel (hH1) into the comparable position of the human skeletal muscle isoform (V754I) confers cardiac-type slow inactivation on the skeletal muscle Na channel isoform (Vilin et al., 2001). Moreover, in the present study a modest decrease in the rate of entry to, and an increase in the rate of recovery from, slow inactivation occurred with the E758C substitution mutation in domain II, further suggesting that structural derangements in the outer pore can destabilize the slow-inactivated state.

Indeed, recent reports support the notion structures around the outer vestibule may undergo a conformational rearrangement during slow inactivation. Benitah et al. (1999) showed that introduction of a double cysteine substitution at two sites in the outer pore (K1237C + W1531C) resulted in an enhanced rate of disulfide bond formation during prolonged conditioning depolarizations designed to induce entry into an early slow inactivation state (I_M) than during shorter conditioning pulses (Benitah et al., 1999). More re-

cently, Ong et al. (2000) demonstrated that a cysteine substitution at residue F1236 in the domain III P-region of rNaV1.4 has reduced accessibility to externally applied MTS-EA when Na channels are slow inactivated compared with nonslow-inactivated controls (Ong et al., 2000). Although F1236 is part of the structure of the outer vestibule, the orientation and location of this site relative to the SS2 segments studied here is not well characterized. The apparent conflict between these experimental results may reflect structural alterations elsewhere in the outer pore that are not detectable in residues COOH-terminal to the selectivity filter. Given the possibility that our assay might overlook modest, more distant P-region conformational rearrangements coupled to slow inactivation, we offer the more conservative interpretation from our data that the aqueous vestibule remains unobstructed in regions COOH-terminal to the selectivity filter during slow inactivation.

Another possibility is that structures in the P-regions might undergo a modest conformational change as an epi-phenomenon of more distant rearrangements, possibly involving the S6 segments, which probably lie closely apposed to the P-regions and converge to form the inner mouth of the pore. In support of this notion, a growing body of evidence has demonstrated the importance of structures lining the internal mouth of the pore in slow inactivation. Several point mutations in S6 segments have profound effects on slow inactivation (Wang and Wang, 1997; Takahashi and Cannon, 1999; O'Reilly et al., 2000, 2001). Recently, our laboratory reported a conformational change accompanying slow inactivation in the S6 segment of domain IV (Vedantham and Cannon, 2000).

This work was supported by grants from the National Institutes of Health: AR42703 to S.C. Cannon from the NIAMS, and K08-NS02137 to A.F. Struyk from the NINDS.

Submitted: 11 July 2002
Revised: 3 September 2002
Accepted: 3 September 2002

REFERENCES

Balser, J.R., H.B. Nuss, N. Chiamvimonvat, M.T. Perez-Garcia, E. Marban, and G.F. Tomaselli. 1996. External pore residue mediates slow inactivation in μ1 rat skeletal muscle sodium channels. *J. Physiol.* 494:431–442.

Benitah, J.P., Z. Chen, J.R. Balser, G.F. Tomaselli, and E. Marban. 1999. Molecular dynamics of the sodium channel pore vary with gating: interactions between P-segment motions and inactivation. *J. Neurosci.* 19:1577–1585.

Cannon, S.C. 1996. Slow inactivation of sodium channels: more than just a laboratory curiosity. *Biophys. J.* 71:5–7.

Chiamvimonvat, N., M.T. Perez-Garcia, R. Ranjan, E. Marban, and G.F. Tomaselli. 1996. Depth asymmetries of the pore-lining segments of the Na+ channel revealed by cysteine mutagenesis. *Neuron.* 16:1037–1047.

Cummins, T.R., and F.J. Sigworth. 1996. Impaired slow inactivation in mutant sodium channels. *Biophys. J.* 71:227–236.

Featherstone, D.E., J.E. Richmond, and P.C. Ruben. 1996. Interaction between fast and slow inactivation in SkM1 sodium channels. *Biophys. J.* 71:3098–3109.

Hayward, L.J., G.M. Sandoval, and S.C. Cannon. 1999. Defective slow inactivation of sodium channels contributes to familial periodic paralysis. *Neurology.* 52:1447–1453.

Jurkat-Rott, K., N. Mitrovic, C. Hang, A. Kouzmekine, P. Iaizzo, J. Herzog, H. Lerche, S. Nicole, J. Vale-Santos, D. Chauveau, et al. 2000. Voltage-sensor sodium channel mutations cause hypokalemic periodic paralysis type 2 by enhanced inactivation and reduced current. *Proc. Natl. Acad. Sci. USA.* 97:9549–9554.

Karlin, A., and M.H. Akabas. 1998. Substituted-cysteine accessibility method. *Methods Enzymol.* 293:123–145.

Khodorov, B., L. Shishkova, E. Peganov, and S. Revenko. 1976. Inhibition of sodium currents in frog ranvier node treated with local anesthetics. Role of slow sodium inactivation. *Biochim. Biophys. Acta.* 433:409–435.

Kuzmenkin, A., V. Muncan, K. Jurkat-Rott, C. Hang, H. Lerche, F. Lehmann-Horn, and N. Mitrovic. 2002. Enhanced inactivation and pH sensitivity of Na(+) channel mutations causing hypokalaemic periodic paralysis type II. *Brain.* 125:835–843.

Liman, E.R., J. Tytgat, and P. Hess. 1992. Subunit stoichiometry of a mammalian K^+ channel determined by construction of multimeric cDNAs. *Neuron.* 9:861–871.

Lipkind, G.M., and H.A. Fozzard. 2000. KcsA crystal structure as framework for a molecular model of the Na(+) channel pore. *Biochemistry.* 39:8161–8170.

Liu, Y., M.E. Jurman, and G. Yellen. 1996. Dynamic rearrangement of the outer mouth of a K+ channel during gating. *Neuron.* 16: 859–867.

McClatchey, A.I., S.C. Cannon, S.A. Slaugenhaupt, and J.F. Gusella. 1993. The cloning and expression of a sodium channel beta 1-subunit cDNA from human brain. *Hum. Mol. Genet.* 2:745–749.

Ong, B.H., G.F. Tomaselli, and J.R. Balser. 2000. A structural rearrangement in the sodium channel pore linked to slow inactivation and use dependence. *J. Gen. Physiol.* 116:653–662.

O'Reilly, J.P., S.Y. Wang, and G.K. Wang. 2000. A point mutation in domain 4-segment 6 of the skeletal muscle sodium channel produces an atypical inactivation state. *Biophys. J.* 78:773–784.

O'Reilly, J.P., S.Y. Wang, and G.K. Wang. 2001. Residue-specific effects on slow inactivation at V787 in D2-S6 of Na(v)1.4 sodium channels. *Biophys. J.* 81:2100–2111.

Perez-Garcia, M.T., N. Chiamvimonvat, E. Marban, and G.F. Tomaselli. 1996. Structure of the sodium channel pore revealed by serial cysteine mutagenesis. *Proc. Natl. Acad. Sci. USA.* 93:300–304.

Rudy, B. 1978. Slow inactivation of the sodium conductance in squid giant axons. Pronase resistance. *J. Physiol.* 283:1–21.

Struyk, A.F., K.A. Scoggan, D.E. Bulman, and S.C. Cannon. 2000. The human skeletal muscle Na channel mutation R669H associated with hypokalemic periodic paralysis enhances slow inactivation. *J. Neurosci.* 20:8610–8617.

Takahashi, M., and S. Cannon. 1999. Enhanced slow inactivation by V445M: a sodium channel mutation associated with myotonia. *Biophys. J.* 76:861–868..

Townsend, C., and R. Horn. 1997. Effect of alkali metal cations on slow inactivation of cardiac Na^+ channels. *J. Gen. Physiol.* 110:23–33.

Vedantham, V., and S. Cannon. 1998. Slow inactivation does not affect movement of the fast inactivation gate in voltage-gated Na^+ channels. *J. Gen. Physiol.* 111:83–93.

Vedantham, V., and S.C. Cannon. 2000. Rapid and slow voltage-dependent conformational changes in segment IVS6 of voltage-gated Na(+) channels. *Biophys. J.* 78:2943–2958.

Vilin, Y.Y., E. Fujimoto, and P.C. Ruben. 2001. A single residue differentiates between human cardiac and skeletal muscle Na+ channel slow inactivation. *Biophys. J.* 80:2221–2230.

Wang, S., and G.K. Wang. 1997. A mutation in segment I-S6 alters slow inactivation of sodium channels. *Biophys. J.* 72:1633–1640.